Journal Pre-proof

MiR-130a-5p/Foxa2 axis modulates fetal lung development in congenital diaphragmatic hernia by activating the Shh/Gli1 signaling pathway

Xue Li, Hao Liu, Yuan Lv, Wenqian Yu, Xiaomei Liu, Caixia Liu

PII: S0024-3205(19)31094-X

DOI: https://doi.org/10.1016/j.lfs.2019.117166

Reference: LFS 117166

To appear in: *Life Sciences*

Received date: 16 September 2019

Revised date: 5 December 2019

Accepted date: 9 December 2019

Please cite this article as: X. Li, H. Liu, Y. Lv, et al., MiR-130a-5p/Foxa2 axis modulates fetal lung development in congenital diaphragmatic hernia by activating the Shh/Gli1 signaling pathway, *Life Sciences*(2019), https://doi.org/10.1016/j.lfs.2019.117166

MiR-130a-5p/Foxa2 axis modulates fetal lung development in congenital diaphragmatic hernia by activating the Shh/Gli1 signaling pathway

Xue Li [a,b], Hao Liu [a,b], Yuan Lv [a,b], Wenqian Yu [a,b], Xiaomei Liu [a,b] and Caixia Liu [a,b] *

[a] Department of Gynecology and Obstetrics, Shengjing Hospital of China Medical University, Shenyang, China

[b] Key Laboratory of Maternal-Fetal Medicine of Liaoning Province, Benxi, China.

*Correspondence: Professor Caixia Liu, 36 Sanhao Street, Shenyang, Liaoning 110004, China.
E-mail: liucx1716@163.com

Abstract

Aims: Congenital diaphragmatic hernia (CDH) is a lethal birth defect characterized by congenital lung malformation, and the severity of pulmonary hypoplasia directly affects the prognosis of infants with CDH. Using a nitrofen-induced CDH rat model, we previously reported that Foxa2 expression was downregulated in CDH lungs by proteomics analysis. Here, we investigate the role of miR-130a-5p/Foxa2 axis in lung development of the nitrofen-induced CDH and evaluate its potential role in vivo prenatal therapy.

Main methods: Nitrofen was orally administrated on embryonic day (E) 8.5 to establish a rat CDH model, and fetal lungs were collected on E13.5, E15.5, E17.5, E19.5 and E21.5. The binding sites of miR-130a-5p on Foxa2 mRNA were identified using bioinformatics prediction software and were validated via luciferase assay. The expression levels of miR-130a-5p and Foxa2 were detected using qRT-PCR, ISH, IHC and western blotting. The role of miR-130a-5p/Foxa2 axis in CDH-associated lung development was investigated in ex vivo lung explants.

Key findings: We found that Foxa2 was downregulated in CDH lung tissues, and Foxa2 upregulating improved CDH branching morphogenesis in ex vivo lung explants. Meanwhile, we also showed that miR-130a-5p was significantly upregulated in CDH lungs and thus inversely correlated with Foxa2. Increasing miR-130a-5p abundance with mimics decreases Foxa2-driven Shh/Gli1 signaling and inhibits branching morphogenesis in ex vivo lung explants.

Significance: This study was the first to show that the miR-130a-5p/Foxa2 axis played a crucial role in CDH-associated pulmonary hypoplasia. These findings may provide relevant insights into the prenatal diagnosis and prenatal therapy of CDH.

Keywords

Congenital diaphragmatic hernia, pulmonary hypoplasia, miRNAs, Foxa2, branching morphogenesis

1. Introduction

Congenital diaphragmatic hernia (CDH) is the incomplete formation of the diaphragm, leading to abdominal organ herniation into the thoracic cavity [1]. The incidence is about 1/2000-3000 live births [2]. At present, the diagnosis and treatment of CDH have matured and become standardized, and most children can get effective treatment [3]. However, CDH-associated pulmonary hypoplasia and pulmonary hypertension increase rates of poor prognosis and mortality [4]. Therefore, it is particularly important to study the molecular mechanism of CDH-associated pulmonary hypoplasia, which can provide a new means of diagnosis and treatment, and effectively improve the prognosis of children with CDH.

Embryonic lung development is a complex coordinated process requiring cell differentiation and interaction between respiratory epithelial cells and the surrounding mesenchymal environment [5]. CDH-associated pulmonary hypoplasia is characterized by fewer effective pulmonary surface areas, fewer distal branches of pulmonary parenchyma and fewer alveoli [6]. The alveolar wall is thickened, and the interstitial components of the lung are abnormal, while compliance is decreased. Morphological characteristics of branching arrest or delay in the pseudoglandular stage of fetal lung development are observed in patients with severe fatal CDH [7]. Several evolutionarily conserved signaling pathways are involved in different stages of embryonic lung development. In particular, fibroblast growth factor, bone morphogenetic protein, wingless secretory glycoprotein (WNT) and Hedgehog/Gli signaling are involved in lung morphogenesis and epithelial differentiation [8,9]. In addition, a good balance and interaction between these signaling pathways and key transcription factors of lung development, including TTF1, GATA6 and Foxa2, are essential for normal lung morphogenesis.

The Foxa transcription factor family has a wide range of functions in embryonic development, cell cycle regulation, glycolipid metabolism, aging, immune regulation and so on [10]. Foxa2 expression in the lungs is limited to a subset of respiratory epithelial cells [11]. Foxa2 is a key transcriptional regulator in airway epithelial cell differentiation and lung development, and it contributes to normal branching and cell commitment [12]. Transcription factors and signaling events mediating early lung formation have been extensively studied. Foxa2 regulates Shh and Shh-dependent genes in respiratory epithelial cells, thereby affecting the expression of genes required for lung branching [13]. We compared the lung tissues of fetal rats with and without CDH by proteomic analysis and found that Foxa2 expression was downregulated in CDH lung tissue. However, the temporal and spatial expression of Foxa2 in CDH lung tissue and its regulatory mechanism in lung development are still unclear.

Although about 10% of CDH patients have chromosomal abnormalities, the genetic causes of 85% of CDH patients are still unclear [14]. The inconsistency of monozygotic twins (one fetal diaphragmatic hernia) also emphasizes the importance of considering epigenetic factors [15]. MicroRNAs (miRNAs) are important epigenetic regulators [16]; they are small RNAs that regulate the expression of target

genes at the post-transcriptional level and are essential for normal organogenesis during embryonic development. Analysis of the expression of miRNAs at different developmental stages of human and rat lung morphogenesis has shown that the function of miRNAs is evolutionarily conserved to some extent [17,18]. Dicer is a key component in the processing of miRNAs, and its inactivation during lung development has been found to lead to inhibition of lung epithelial branching [19]. Keijzer et al. found that miRNA-200b was increased in abnormally developed lung tissues of children with CDH. In subsequent animal experiments, this group demonstrated that prenatal intrauterine intervention with miRNA-200b improved lung development and lowered CDH incidence [20]. miRNAs regulating the activity of Foxa2 are considered major molecular mediators in lung development.

In the present study, we evaluated miR-130a-5p as a specific regulator of Foxa2 expression in epithelial cells during CDH lung development. Using a loss- and gain-of-function approach, we analyzed the role of the miR-130a-5p/Foxa2 axis in ex vivo lung explants.

2. Materials and Methods

2.1. Bioinformatics Prediction

Three types of bioinformatics software, TargetScan (http://www.targetscan.org/), miRDB (http://mirdb.org/) and DIANA (diana.imis.athena-innovation.gr), were used to predict miRNAs with potential binding sites on Foxa2 mRNA.

2.2. CDH Rat Model

Our study was approved by the Animal Research Committee of China Medical University. Sprague Dawley rats were provided by Liaoning Changsheng Biotechnology, and were maintained according to the "Guide to the Care and Use of Experimental Animals." The animals were mated at night, and the next day was considered embryonic day zero (E0). On E9, pregnant rats were administered either 100 mg nitrofen (N141413; Aladdin, Shanghai, China) in olive oil or olive oil alone [21]. On E13.5, E15.5, E17.5, E19.5 and E21.5, fetuses were removed by cesarean section to examine the diaphragm and harvest the lungs under the microscope. Fetuses were divided into two groups, the control group (CON) exposed to olive oil only, while the CDH group (CDH) was exposed to nitrofen and had CDH. During embryonic development in rat, the diaphragm is completely closed on E17. Regarding this experimental design, the occurrence of diaphragmatic hernia could not be determined on E13 and E15. Therefore, for this early gestational age, CDH group refers to the fetuses exposed to nitrofen (independently of CDH development). Lungs were either stored at -80℃ or fixed in 4% paraformaldehyde.

2.3. RNA Extraction and Quantitative qRT-PCR

Total RNA was extracted from fetal lung tissues or cells with RNAiso Plus extraction reagent (Takara, Beijing, China). After measurement of the RNA concentration, cDNA corresponding to the mRNAs was reverse transcribed using PrimeScript™ RT reagent kit with gDNA Eraser (Takara), and SYBR® Premix Ex Taq™ II (Takara) was used to

perform quantitative real-time PCR (qRT-PCR) according to the manufacturer's instructions. cDNA corresponding to the miRNAs was reverse transcribed using miRNA 1st Strand cDNA Synthesis Kit (Vazyme, Nanjing, China), and miRNA Universal SYBR qPCR Master Mix (Vazyme, Nanjing, China) was used to perform qRT-PCR according to the manufacturer's instructions. The specific mRNA PCR primers were designed by Sangon Biotech Co. Ltd. (Shanghai, China), as described in Supplementary Table S1. Specific miRNA PCR primers were designed by RiboBio (Guangzhou, China). β-Actin and U6 were used as internal controls to determine fold-changes by the 2-ΔΔCt method.

2.4. Western Blotting

Total protein was extracted using a protein extraction kit (Beyotime Biotechnology, Shanghai, China). Protein was separated by 10% sodium dodecyl sulfate (SDS)-polyacrylamide gel electrophoresis (PAGE) and transferred to polyvinylidene fluoride (PVDF) membranes (Millipore, MA, USA). The membranes were incubated with primary antibody overnight at 4℃(the primary antibodies listed in Supplementary Table S2) and then with secondary antibody for 2 hours at room temperature. After being washed, the bands were visualized using Quantity One imaging software (Bio-Rad, CA, USA).

2.5. Immunohistochemistry (IHC), Immunofluorescence (IF) and in situ hybridization (ISH)

The paraffin- embedded lungs (2.5- μm sections) were deparaffinized in dimethylbenzene and hydrated in an ethanol series. After heat repair and endogenous enzyme blocking, IHC and IF was performed using the streptavidin- peroxidase method (OriGene Technologies, Beijing, China) according to the kit protocol. The primary antibodies are listed in Supplementary Table S2. For in situ hybridization (ISH), the experiments were performed according to the kit instructions (Boster Biological Technology, Nanjing, China), and the digoxigenin-labeled oligonucleotide miR-130a-5p detection probe sequence was as follows: (5′-3′) AGTAGCACAATGTGAAAAGA.

2.6. Fetal Lung Explant Culture

The fetal lungs were isolated from E13.5 embryos, transferred to Costar Transwell cells (Corning Incorporated, Corning, NY, USA), and cultured at the air- liquid interface in serum- free DMEM/F12 medium (Biological Industries). The explants were treated with 200 nM miR-NC, miR-130a-5p mimic and miR-130a-5p inhibitor (GenePharma, Shanghai, China) or recombinant Foxa2 (R&D Systems, MN, USA), and cultured for 4 days. The miRNA and protein treatments were repeated every 24 hours. Branching morphogenesis, number of peripheral airway buds and explant surface were monitored daily. The differences between day 0 and day 4 of culture were expressed as the D4/D0 ratio. After 96 hours, the lungs were harvested for RNA and protein isolation. The sequences of RNA mimic/inhibitor are listed in Supplementary Table S3.

2.7. Cell Culture

HEK293T cells (human embryonic kidney cells; Institute of Biochemistry and Cell Biology, Chinese Academy of Sciences, Shanghai, China) and BEAS-2B cells (human bronchial epithelial cells; Chinese Academy of Sciences, Shanghai, China, Manassas, VA) were maintained in high-glucose DMEM (Biological Industries). Fetal bovine serum (FBS, 10%) (Biological Industries), 50 IU/mL penicillin, and 50 ug/mL streptomycin (Invitrogen, Carlsbad, CA, USA) were added to the culture medium. All cells were grown at 37℃in a humidified incubator in 5% CO2.

2.8. Luciferase Assay

HEK293T cells were seeded in 96-well plates. The cells were co-transfected with 5 nmol of miR-130a-5p mimic or scrambled NC (GenePharma) and 100 ng of wild-type or mutant dual-luciferase reporter vector carrying a Foxa2 gene fragment (pmiR-RB-Report-Foxa2) (GenePharma) using Lipofectamine 3000. At 48 hours post-transfection, luciferase activity was measured using the Dual-Luciferase Reporter Assay System (Promega,Madison, WI, USA) according to the manufacturer's protocol.

2.9. EdU Proliferation Assay

5-ethynyl-2′-deoxyuridine (EdU) was added to ex vivo lung explant cultures, and the tissue was incubated for 4 hours before harvesting. After fixing, a click reaction was performed according to the manufacturer's protocol (C0078S, Beyotime, Beijing, China). The positive rate was determined by Image Pro Plus 6.

2.10. Statistical Analysis

Data are presented as means ± SD of three independent experiments. Statistical analyses were performed with GraphPad Prism 6.0 software (La Jolla, CA). Statistical comparison of experimental groups was done using the unpaired Student t- test or one- way analysis of variance. $P < 0.05$ was considered statistically significant.

3. Results

3.1. Temporal and Spatial Expression of Foxa2 in CDH Fetal Lung Tissues

The gene expression of Foxa2 was determined in CDH and control fetal lung tissues during lung development by qRT-PCR. There was no significant difference at E15.5, while the expression of Foxa2 decreased significantly in CDH lung tissues at E17.5, E19.5 and E21.5 (Figure 1A). Western blot analysis also showed that the difference in protein expression between the two groups was more evident in later embryonic age (Figure 1B).The IHC results indicated that Foxa2 was consistently expressed in epithelial cells at different stages of lung development and that the expression level was lower in the CDH group than control group (Figure 1C).

In late embryonic development, the expression of Foxa2 was significantly lower in the distal epithelium at the canalicular (E19.5) and saccular (E21.5) stages in CDH group (Figure 1C). Immunofluorescence double staining at E21.5 showed that the expression of bronchia epithelial markers (CCSP) and alveoli epithelial markers (SP-C) decreased in the distal lung epithelial cells of CDH (Figure 2A), and western blot analysis also confirmed this result (Figure 2C and D). H&E staining at E21.5 showed that CDH lungs have fewer alveoli and thicken lung parenchyma (Figure 2B). IHC

staining showed decreased levels of proliferation markers (PCNA and Ki-67) in CDH lung epithelial cells (Figure 2B), which consistent with the western blot results (Figure 2C and D). In addition to cell proliferation, cell apoptosis-related proteins, Bax and Bcl2 were also dectected and showed increased expression levels in CDH lungs (Figure 2C and D). To summarize, Foxa2 downregulated in CDH lungs, associated with decreased cell proliferation, increased apoptosis and reduced differentiation of the distal airway epithelium.

3.2. Effect of Foxa2 on Branching Morphogenesis in Ex Vivo Lung Explants

Ex vivo lung explants were used to clarify the role of Foxa2 in the development of fetal lungs in nitrofen-induced CDH (Figure 3A-D). We dissected control and CDH rat lungs at E13.5, and CDH lungs were incubated with 0.01 μg/ml of recombinant Foxa2. The expression level of Foxa2 was evaluated by western blot after treated with recombinant protein (Figure 3E). Peripheral airway buds and lung explant surface were evaluated at day 0 (D0) and day 4 (D4), and these were significantly lower in the CDH group than control group, while treatment of CDH with recombinant Foxa2 promoted the formation of peripheral airway buds and lung explant surface (Figure 3B and C). EdU staining in cultured lungs showed that the proliferation of tip distal lung epithelium was weaker in the CDH group, while the proliferation level increased after treatment with recombinant Foxa2 (Figure 3D). Meanwhile, western blot analysis showed that the treatment of Foxa2 recombinant protein increased lung differentiation and decreased apoptosis in CDH group (Figure 3F and G).

3.3. Expression of MiR-130a-5p is High in CDH Fetal Lung Tissues, and Foxa2 is a MiR-130a-5p Target

The results of the three bioinformatics prediction programs (TargetScan, miRDB and DIANA) simultaneously identified 4 miRNAs that potentially bind to Foxa2 (Figure 4A). And we showed all miRNAs and scores predicted by the three bioinformatic software in Supplementary Table S4. We then co-transfected HEK293T cells with these 4 miRNAs and wild-type (WT) dual-luciferase vector-mediated Foxa2 constructs and performed the dual-luciferase assays. We found that miR-130a-5p and miR-876 exhibited a strong interaction with Foxa2 (Figure 4B). The expression levels of miR-130a-5p and miR-876 were determined in fetal lung tissues of the control and CDH groups using qRT-PCR. MiR-876 expression showed no significant differences between control and CDH fetal lung tissues (Supplementary Figure S1). On the other hand, miR-130a-5p was significantly upregulated in CDH fetal lung tissues compared with control group during lung development (Figure 4C). We performed in situ hybridization to evaluate the tissue distribution of miR-130a-5p in control and CDH lungs (Figure 4G). During the canalicular (E19.5) and saccular (E21.5) stages of lung development, the expression of miR-130a-5p was higher in the proximal epithelial lining of the large airways compared to the epithelial cells in the distal terminal saccules. We observed higher miR-130a-5p expression in CDH fetal lungs (Figure 4G).

The results of bioinformatics predictions indicated one site that could interact with miR-130a-5p. Luciferase assays were conducted to ascertain whether Foxa2 could

directly target miR-130a-5p via these putative binding sites (Figure 4D). The luciferase activity of the miR-130a-5p and Foxa2 WT co-transfected group was greatly reduced compared with other groups (Figure 4E). Meanwhile, Foxa2 expression was significantly decreased when BEAS-2B cells were transfected with miR-130a-5p mimic (Figure 4F), which indicates that Foxa2 expression is likely regulated by miR-130a-5p.

3.4. Introducing MiR-130a-5p Inhibitor Corrects CDH-associated Abnormal Branching Morphogenesis in Ex Vivo Lung Explants

To investigate if miR-130a-5p can directly affect lung branching morphogenesis in control or CDH fetal lungs, we performed ex vivo lung explant culture (Figure 5A-C). We incubated control rat lungs (at E13.5) with 200 nM of either negative control miRNA (miR-NC) or miR-130-5p mimic. And the lungs from the CDH group were incubated with 200 nM of miR-130a-5p inhibitor or negative control. Lung explant surface and peripheral airway buds were evaluated at day 0 (D0) and day 4 (D4). MiR-130a-5p mimic decreased D4/D0 of the total number of peripheral airway buds and lung explant surface indicating a direct inhibitory effect of increased miR-130a-5p expression on airway branching. The treatment of CDH lung explants with miR-130a-5p inhibitor improved the formation of peripheral airway buds and lung explant surface (Figure 5A-C). To ensure transfection efficiency, qRT-PCR was used to determine the expression of miR-130a-5p after lung explant cultures (Figure 5D). Western blot analysis also showed that miR-130a-5p mimic reduced lung differentiation and increased apoptosis in control group, and miR-130a-5p inhibitor increased lung differentiation and decreased apoptosis in CDH group (Figure 5E and F).

3.5. MiR-130a-5p Regulates Foxa2-Driven SHH Signaling in Ex Vivo Lung Explants

To further clarify the mechanism by which the miR-130a-5p-Foxa2 axis regulates lung morphogenesis in nitrofen-induced CDH rats, we dissected CDH rat lungs at E13.5, and incubated them with miR-130a-5p mimic and/or recombinant Foxa2 protein for 96 hours. We found that recombinant Foxa2 promoted lung branching morphogenesis. When miR-130a-5p mimic and recombinant Foxa2 protein were added to the culture medium at the same time, lung branching was inhibited to some extent (Fig. 6A-C). Western blot analysis was performed on the cultured lung tissues. Activation of the Shh signaling pathway was detected by measuring the protein expression of Shh and Gli1. In the CDH group, the expression of Shh and Gli1 was low (Fig. 6D line1 and E), but it increased after treatment with recombinant Foxa2 protein (Fig. 6D line2 and E). Interestingly, when miR-130a-5p mimic was added to the lung explant culture treated with recombinant Foxa2 protein, Foxa2 expression was reduced and the activation of the SHH signaling pathway was inhibited (Fig. 6D line3 and E). RT-PCR was performed to determine the gene expression of Foxa2, Shh and Gli1, and the results were consistent with protein expression findings (Fig. 6F).

4. Discussion

Our protein expression profiles from CDH fetal lung tissue in the pseudoglandular to canalicular stages of lung development revealed several differentially expressed proteins and signing pathways. In the present research, the downregulated Foxa2 and Shh signaling pathways were further studied, and miR-130a-5p was predicted and verified as an epigenetic regulator of Foxa2. We found that miR-130a-5p inhibitor and recombinant Foxa2 protein can improve CDH lung branching morphogenesis in ex vivo lung explants. When miR-130a-5p expression is increased in vitro, Shh/Gli1 signaling is inhibited and the expression of miR-130a-5p target Foxa2 decreases.

Foxa2 is a key transcription factor in lung development, and its expression is limited to a subset of respiratory epithelial cells. Previous in vitro studies have found that Foxa2 enhances the expression of CCSP [22] and TTF-1 and SP-C [23], supporting its potential role in regulating gene expression and differentiation in respiratory epithelial cells. To our knowledge, this is the first report on the function of Foxa2 in CDH-associated pulmonary hypoplasia. Our results showed that Foxa2 expression was downregulated in CDH lung tissues, and IHC results indicated that Foxa2 was localized in respiratory epithelial cells. We also found that the expression of Foxa2 in the distal epithelium decreased significantly in CDH at the canalicular (E19.5) and saccular (E21.5) stages (Figure 1C). *Whitsett et al.* demonstrated that the ectopic expression of Foxa2 in the distal respiratory epithelial cells impairs the branching and differentiation of peripheral lung epithelial cells in the late stage of lung development [12]. The expression of bronchia epithelial markers (CCSP) and alveoli epithelial markers (SP-C) in fetal respiratory epithelium was determined by immunofluorescence double staining (Figure 2A). A decreased level of cell proliferation and increased level of cell apoptosis were also observed in CDH lungs (Figure 2B-D). Our results demonstrated that Foxa2 is required for normal lung develoment, and the differentiation defect of the distal airway epithelium in CDH lungs associated with the downregulated of Foxa2.

To further clarify the effect of Foxa2 on the lung branching, we simulated the in vivo environment in in vitro lung tissue cultures at E13.5 [24]. After 96 hours of culture, we found that lung branching in the CDH group was significantly delayed. These results are consistent with the findings of *Keijzer et al.* [25]. Our results also showed that increasing Foxa2 expression in fetal lung explants with recombinant protein treatment led to improved branching morphogenesis in the CDH group (Fig. 3A-C). EdU staining in cultured lungs showed that the proliferation of tip distal lung epithelium was weaker in the CDH group, while the proliferation level increased after treatment with recombinant Foxa2 (Figure 3D). Meanwhile, increasing expression level of Foxa2 can improve lung differentiation and inhibit apoptosis in CDH group (Figure 3F and G). Therefore, in the CDH group, the downregulation of Foxa2 expression may impair the differentiation of distal lung epithelial cells and lung branching.

MiRNAs are a class of non-coding small RNAs that target mRNA and have post-transcriptional gene regulatory activity. Some significant progress has been made in understanding the role of miRNAs in lung development and the pathogenesis of lung

diseases [26]. Mice conditionally knocked out for dicer in pulmonary epithelial cells showed impaired epithelial branching, emphasizing the important regulatory role of miRNAs in pulmonary epithelial morphogenesis. Keijzer et al. were the first to report that miRNA can be used to treat CDH and related pulmonary dysplasia through the placental barrier [27]. In the present study, miR-130a-5p was predicted by bioinformatics software (TargetScan, miRDB and DIANA) to be able to bind to the 3'-UTR of Foxa2 as demonstrated by the dual-luciferase reporter assay. MiRNA-130a is a vertebrate-specific miRNA, which is widely used in angiogenesis and the cell cycle [28]. The miR-130/301 family is the main regulator of hypoxic pulmonary hypertension cell proliferation [29]. In this study, we demonstrated that the expression of miR-130a-5p is high in the CDH group and observed in the respiratory epithelium during lung development. We also demonstrated earlier that the expression level of Foxa2 was decreased after overexpression of miR-130a-5p in human bronchial epithelial cells. These results indicate that Foxa2 is a target gene of miR-130a-5p in CDH lung development. To investigate the role of miR-130a-5p in CDH lung development, miRNA was added to the culture medium in vitro. MiR-130a-5p mimic inhibited the development of control lung branching, while mir-130a-5p inhibitor promoted the development of branching in the CDH group (Figure 5A-C). Mir-130a-5p and Foxa2 had opposite effects on the development of lung branching in ex vivo lung explants.

To further explore the mechanism of the miR-130a-5p/Foxa2 axis in the development of pulmonary branching, mir-130a-5p mimic and recombinant Foxa2 protein were added to the CDH culture medium (Figure 6A-C). MiR-130a-5p mimic inhibited the improvement of branching by recombinant Foxa2 protein in the CDH group. Gli zinc finger proteins Gli1, Gli2 and Gli3 are the main transcription factors mediating Shh signaling. Gli1 is the transcriptional target of the Shh pathway [30], which plays a transcriptional activation role in response to Shh signaling [31]. Foxa2 can negatively regulate several components of the Shh signaling pathway by binding to the same enhancer region, thereby inhibiting the expression of Gli1 and some common Gli1 upregulated target genes [32]. In this study, the cultured lung tissue results showed that Foxa2 overexpression activated Shh/Gli1 signaling pathway activity, while miR-130a-5p negatively regulated this process by binding to Foxa2.

MiR-130a-5p mimic and Foxa2 recombinant significantly improved lung branching morphology in the CDH rat model cultured in vitro, but the effect of prenatal intervention in vivo needs to be further studied. To determine the optimal dose and time of miR-130a-5p in prenatal treatment, levels and metabolism of miR-130a-5p need to be further studied in cell experiments.

5. Conclusions

Our findings demonstrated that miR-130a-5p/Foxa2 axis play a crucial role in pulmonary hypoplasia of the nitrofen-induced CDH rat model. Furthermore, we observed that upregulating Foxa2 with recombinant protein improved lung branching

morphogenesis in ex vivo explants in CDH group, which was inversely correlated with increasing miR-130a-5p abundance. Ultimately, these findings indicate that miR-130a-5p/Foxa2 axis may be a potential target in vivo prenatal therapy to improve abnormal lung development in CDH.

Funding: The present study was supported by the major project of National Health and Family Planning commission of China (grant no. 201402006).

Acknowledgments: We appreciate BioMed Proofreading for editing the manuscript.

Conflicts of Interest: The authors declare no conflict of interest.

Figure 1. Temporal and spatial expression of Foxa2 in the lungs of the CDH and CON groups. (A) mRNA levels of Foxa2 in developing lungs were determined by qRT-PCR and results were expressed relative to the control at E15.5, E17.5, E19.5 and E21.5. (B) Representative immunoblots and densitometric analysis of expression of Foxa2 proteins in the fetal lungs at E15.5, E17.5, E19.5 and E21.5. Results were normalized relative to the expression of β-Actin. (C) Representative photomicrographs of IHC staining for Foxa2 in the lung sections from CON and CDH groups at five gestational stages: E13.5, E15.5, E17.5, E19.5 and E21.5 days. Foxa2 exhibited marked epithelial expression. The expression of Foxa2 was lower in the CDH group than in the CON group. Original magnification, x200, scale bar=100 μm. All results are presented as the mean ± standard error of the mean. * $P<0.05$, and all n= 6 per group.

Figure 2. Characterization of distal lung defects in in CDH lung at E21.5. (A) Immunostaining for E-cadherin shows a decrease in distal epithelium in CDH compared to control. Fluorescent co-labeling of CCSP (green), SP-C (green) and Foxa2 (red) was used to determine the localization of Foxa2, and cell type specific markers reveal defects of distal lung that large decreases in the bronchial epithelium (CCSP) and alveolar epithelium (SP-C) in CDH lung. All images are displayed at 400× magnification. Scale bars: 50 μm. (B) H&E staining shows less saccule formation and thickening of the lung perenchyma in CDH compared CON. IHC staining shows decreased expression levels of PCNA and Ki-67 in CDH lung epithelial cells. (C) and (D) Protein extracts from the CDH and CON lungs were analyzed by western blot using the differentiation and apoptosis antibodies. β-Actin was used as loading control. * $P<0.05$, Student's t test, n=6 per group.

Figure 3. Increased Foxa2 partially rescued the CDH-associated pulmonary hypoplasia phenotype. (A) Lung explant culture of CDH lungs treated with Foxa2 recombinant protein. The upper panel is representative of lung explants at Day Zero and the bottom panel represents lung explants treated with Foxa2 recombinant protein for 4 days. Scale bars, 500 μm. (B) The number of peripheral airway buds and (C) the surface of explant lung was significantly decreased in CDH group, and it can be partially increased when treated with Foxa2

recombinant protein. (D) EdU staining in cultured lungs showed that the proliferation of tip distal lung epithelium was weaker in the CDH group, while the proliferation level increased after treatment with recombinant Foxa2. Scale bars, 500 μm. (E) Foxa2 expression is significantly upregulated in CDH lungs treated with Foxa2 recombinant protein. (F) and (G) Protein extracts from the lung explants treated as in A were analyzed by western blot using the differentiation and apoptosis antibodies. (D0: Day Zero) (D4: Day 4), * $P < 0.05$, 1-way ANOVA, n=9 lungs per group.

Figure 4. Foxa2 is a target of miR-130a-5p. (A) A total of 4 miRNAs were predicted to have potential binding site with Foxa2 by bioinformatics programs. (B) Among the 4 miRNAs co-transfected with the reporter vector Foxa2-WT in HEK293T cells, the relative luciferase activities of 2 miRNAs were most inhibited. (C) MiR-130a-5p was downregulated in CDH lung tissues compared with control tissues via qRT-PCR during lung development. (D) and (E) Predicted miR-130a-5p binding sites in the 3'-UTR of wild-type (Foxa2-WT-3'UTR) and mutant (Foxa2-Mut-3'UTR) Foxa2 sequences. Luciferase reporter assay using HEK293T cells co-transfected with Foxa2-WT (or Foxa2-Mut) and miR-130a-5p mimic. (F) Foxa2 expression was significantly decreased when transfected with mir-130a-5p mimic in BEAS-2B cells. (G) In situ hybridization detected the tissue distribution of miR-130a-5p in control and CDH lungs at E19.5 and E21.5. Scale bars, 500 μm. All data are presented as the mean ± SEM, * P<0.05, ** P<0.01, and n=5 per group.

Figure 5. MiR-130a-5p effects branching morphogenesis in CDH lung development. (A) Lung explant culture of control lungs treated with miR-130a-5p mimic, and CDH lungs treated with miR-130a-5p inhibitor. The upper panel is representative of lung explants at Day Zero and the bottom panel represents lung explants treated with the miR-130a-5p mimic/inhibitor for 4 days. Scale bars, 500 μm. (B) and (C) The number of peripheral airway buds and the surface of explant lung was significantly decreased in CON lungs transfected with miR-130a-5p mimic, and introducing miR-130a-5p inhibitor can normalize CDH abnormal branching morphogenesis. (D) MiR-130a-5p expression is significantly upregulated in control lungs treated with miR-130a-5p mimic, while the expression is significantly downregulated in CDH lungs treated with miR-130a-5p inhibitor. (E) and (F) Protein extracts from the lung explants treated as in A were analyzed by western blot using the differentiation and apoptosis antibodies. (D0: Day Zero) (D4: Day 4), * $P < 0.05$, 1-way ANOVA, n=9 lungs per group.

Figure 6. MiR-130a-5p regulate Foxa2-driven Shh/Gli1 signaling in ex vivo lung explants. (A) CDH embryonic lung explants were treated with control or Foxa2 recombinant protein together with the miR-130a-5p mimic for 4 days. Scale bars, 500 μm. (B) and (C) The number of peripheral airway buds and the surface of explant lung were quantified. (D) and (E) Protein extracts from the lung explants treated as in A were analyzed by western blot using the Shh/Gli1 antibodies. (F) Expression analysis of the indicated genes by quantitative RT-PCR in embryonic lung explants that were treated as in A. (D0: Day Zero) (D4: Day 4), * $P < 0.05$, 1-way ANOVA, n=9 lungs per group.

References:

1. Langham, M.J.; Kays, D.W.; Ledbetter, D.J.; Frentzen, B.; Sanford, L.L.; Richards, D.S., Congenital diaphragmatic hernia. Epidemiology and outcome, CLIN PERINATOL. 23 (1996) 671-88.
2. Pober, B.R., Overview of epidemiology, genetics, birth defects, and chromosome abnormalities associated with CDH, Am J Med Genet C Semin Med Genet. 145C (2007) 158-71.
3. Puligandla, P.S.; Skarsgard, E.D.; Offringa, M.; Adatia, I.; Baird, R.; Bailey, M.; Brindle, M.; Chiu, P.; Cogswell, A.; Dakshinamurti, S.; Flageole, H.; Keijzer, R.; McMillan, D.; Oluyomi-Obi, T.; Pennaforte, T.; Perreault, T.; Piedboeuf, B.; Riley, S.P.; Ryan, G.; Synnes, A.; Traynor, M., Diagnosis and management of congenital diaphragmatic hernia: a clinical practice guideline, CMAJ. 190 (2018) E103-E112.
4. Ameis, D.; Khoshgoo, N.; Keijzer, R., Abnormal lung development in congenital diaphragmatic hernia, SEMIN PEDIATR SURG. 26 (2017) 123-128.
5. Burri, P.H., Structural Aspects of Postnatal Lung Development-Alveolar Formation and Growth, NEONATOLOGY. 89 (2006) 313-322.
6. Donahoe, P.K.; Longoni, M.; High, F.A., Polygenic Causes of Congenital Diaphragmatic Hernia Produce Common Lung Pathologies, AM J PATHOL. 186 (2016) 2532-43.
7. Areechon, W.; Reid, L., Hypoplasia of Lung with Congenital Diaphragmatic Hernia, BMJ. 1 (1963) 230-233.
8. Warburton, D.; Schwarz, M.; Tefft, D.; Flores-Delgado, G.; Anderson, K.D.; Cardoso, W.V., The molecular basis of lung morphogenesis, Mech Dev. 92 (2000) 55-81.
9. Cardoso, W.V.; Lu, J., Regulation of early lung morphogenesis: questions, facts and controversies, DEVELOPMENT. 133 (2006) 1611-24.
10. Maier, J.A.; Lo, Y.; Harfe, B.D., Foxa1 and Foxa2 are required for formation of the intervertebral discs, PLOS ONE. 8 (2013) e55528.
11. Zhou, L.; Lim, L.; Costa, R.H.; Whitsett, J.A., Thyroid transcription factor-1, hepatocyte nuclear factor-3beta, surfactant protein B, C, and Clara cell secretory protein in developing mouse lung, J HISTOCHEM CYTOCHEM. 44 (1996) 1183-93.
12. Zhou, L.; Dey, C.R.; Wert, S.E.; Yan, C.; Costa, R.H.; Whitsett, J.A., Hepatocyte nuclear factor-3beta limits cellular diversity in the developing respiratory epithelium and alters lung morphogenesis in vivo, Dev Dyn. 210 (1997) 305-14.
13. Zhou, X.; Ma, C.; Hu, B.; Tao, Y.; Wang, J.; Huang, X.; Zhao, T.; Han, B.; Li, H.; Liang, C.; Chen, Q.; Li, F., FoxA2 regulates the type II collagen-induced nucleus pulposus-like differentiation of adipose-derived stem cells by activation of the Shh signaling pathway, FASEB J. (2018) fj201800373R.
14. Veenma, D.C.; de Klein, A.; Tibboel, D., Developmental and genetic aspects of congenital diaphragmatic hernia, Pediatr Pulmonol. 47 (2012) 534-45.
15. Pober, B.R.; Lin, A.; Russell, M.; Ackerman, K.G.; Chakravorty, S.; Strauss, B.; Westgate, M.N.; Wilson, J.; Donahoe, P.K.; Holmes, L.B., Infants with Bochdalek

diaphragmatic hernia: sibling precurrence and monozygotic twin discordance in a hospital-based malformation surveillance program, AM J MED GENET A. 138A (2005) 81-8.

16. Inui, M.; Martello, G.; Piccolo, S., MicroRNA control of signal transduction, Nat Rev Mol Cell Biol. 11 (2010) 252-63.
17. Khoshgoo, N.; Kholdebarin, R.; Iwasiow, B.M.; Keijzer, R., MicroRNAs and lung development, Pediatr Pulmonol. 48 (2013) 317-23.
18. Dong, J.; Jiang, G.; Asmann, Y.W.; Tomaszek, S.; Jen, J.; Kislinger, T.; Wigle, D.A., MicroRNA networks in mouse lung organogenesis, PLOS ONE. 5 (2010) e10854.
19. Harris, K.S.; Zhang, Z.; McManus, M.T.; Harfe, B.D.; Sun, X., Dicer function is essential for lung epithelium morphogenesis, Proc Natl Acad Sci U S A. 103 (2006) 2208-13.
20. Pereira-Terra, P.; Deprest, J.A.; Kholdebarin, R.; Khoshgoo, N.; DeKoninck, P.; Munck, A.A.; Wang, J.; Zhu, F.; Rottier, R.J.; Iwasiow, B.M.; Correia-Pinto, J.; Tibboel, D.; Post, M.; Keijzer, R., Unique Tracheal Fluid MicroRNA Signature Predicts Response to FETO in Patients With Congenital Diaphragmatic Hernia, ANN SURG. 262 (2015) 1130-40.
21. Allan, D.W.; Greer, J.J., Pathogenesis of nitrofen-induced congenital diaphragmatic hernia in fetal rats, J Appl Physiol (1985). 83 (1997) 338-47.
22. Bingle, C.D.; Gitlin, J.D., Identification of hepatocyte nuclear factor-3 binding sites in the Clara cell secretory protein gene, BIOCHEM J. 295 (Pt 1) (1993) 227-32.
23. Bohinski, R.J.; Di Lauro, R.; Whitsett, J.A., The lung-specific surfactant protein B gene promoter is a target for thyroid transcription factor 1 and hepatocyte nuclear factor 3, indicating common factors for organ-specific gene expression along the foregut axis, MOL CELL BIOL. 14 (1994) 5671-81.
24. Del, M.P.; Warburton, D., Explant culture of mouse embryonic whole lung, isolated epithelium, or mesenchyme under chemically defined conditions as a system to evaluate the molecular mechanism of branching morphogenesis and cellular differentiation, Methods Mol Biol. 633 (2010) 71-9.
25. Keijzer, R.; Liu, J.; Deimling, J.; Tibboel, D.; Post, M., Dual-hit hypothesis explains pulmonary hypoplasia in the nitrofen model of congenital diaphragmatic hernia, AM J PATHOL. 156 (2000) 1299-306.
26. Sessa, R.; Hata, A., Role of microRNAs in lung development and pulmonary diseases, PULM CIRC. 3 (2013) 315-28.
27. Khoshgoo, N.; Kholdebarin, R.; Pereira-Terra, P.; Mahood, T.H.; Falk, L.; Day, C.A.; Iwasiow, B.M.; Zhu, F.; Mulhall, D.; Fraser, C.; Correia-Pinto, J.; Keijzer, R., Prenatal microRNA miR-200b Therapy Improves Nitrofen-induced Pulmonary Hypoplasia Associated With Congenital Diaphragmatic Hernia, ANN SURG. 269 (2019) 979-987.
28. Xiao, F.; Yu, J.; Liu, B.; Guo, Y.; Li, K.; Deng, J.; Zhang, J.; Wang, C.; Chen, S.; Du Y; Lu, Y.; Xiao, Y.; Zhang, Z.; Guo, F., A novel function of microRNA 130a-3p in hepatic insulin sensitivity and liver steatosis, DIABETES. 63 (2014) 2631-42.
29. Bertero, T.; Cottrill, K.; Krauszman, A.; Lu, Y.; Annis, S.; Hale, A.; Bhat, B.; Waxman, A.B.; Chau, B.N.; Kuebler, W.M.; Chan, S.Y., The microRNA-130/301 family controls

vasoconstriction in pulmonary hypertension, J BIOL CHEM. 290 (2015) 2069-85.

30. Bai, C.B.; Auerbach, W.; Lee, J.S.; Stephen, D.; Joyner, A.L., Gli2, but not Gli1, is required for initial Shh signaling and ectopic activation of the Shh pathway, DEVELOPMENT. 129 (2002) 4753-61.
31. Shi, X.; Zhan, X.; Wu, J., A positive feedback loop between Gli1 and tyrosine kinase Hck amplifies shh signaling activities in medulloblastoma, ONCOGENESIS. 4 (2015) e176.
32. Metzakopian, E.; Lin, W.; Salmon-Divon, M.; Dvinge, H.; Andersson, E.; Ericson, J.; Perlmann, T.; Whitsett, J.A.; Bertone, P.; Ang, S.L., Genome-wide characterization of Foxa2 targets reveals upregulation of floor plate genes and repression of ventrolateral genes in midbrain dopaminergic progenitors, DEVELOPMENT. 139 (2012) 2625-34.

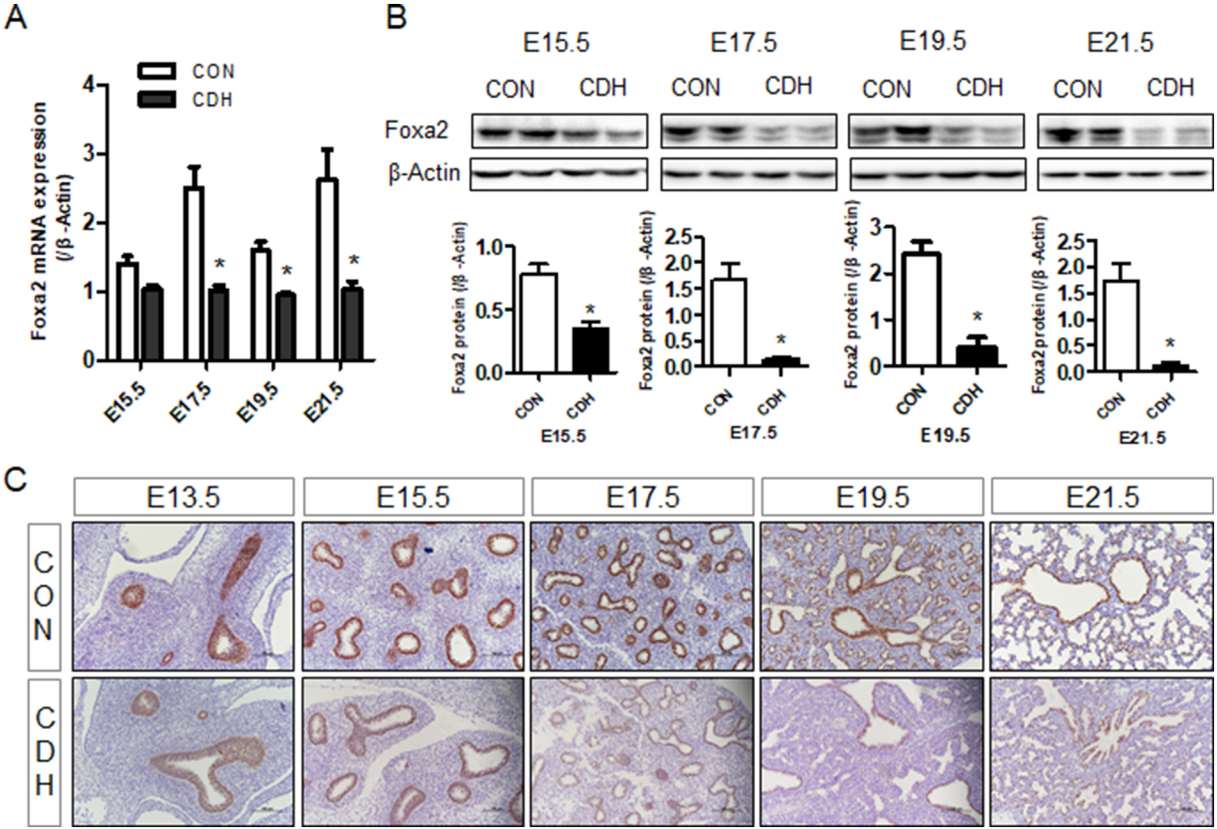
A
CON
CDH
Foxa2 mRNA expression (/β -Actin)
4
3
2
1
0
*
*
*
E15.5
E17.5
E19.5
E21.5
B
E15.5
E17.5
E19.5
E21.5
CON
CDH
Foxa2
β-Actin
Foxa2 protein (/β -Actin)
1.0
0.5
0.0
2.5
2.0
1.5
1.0
0.5
0.0
3
2
1
0
C
E13.5
E15.5
E17.5
E19.5
E21.5
CON
CDH

Figure 1

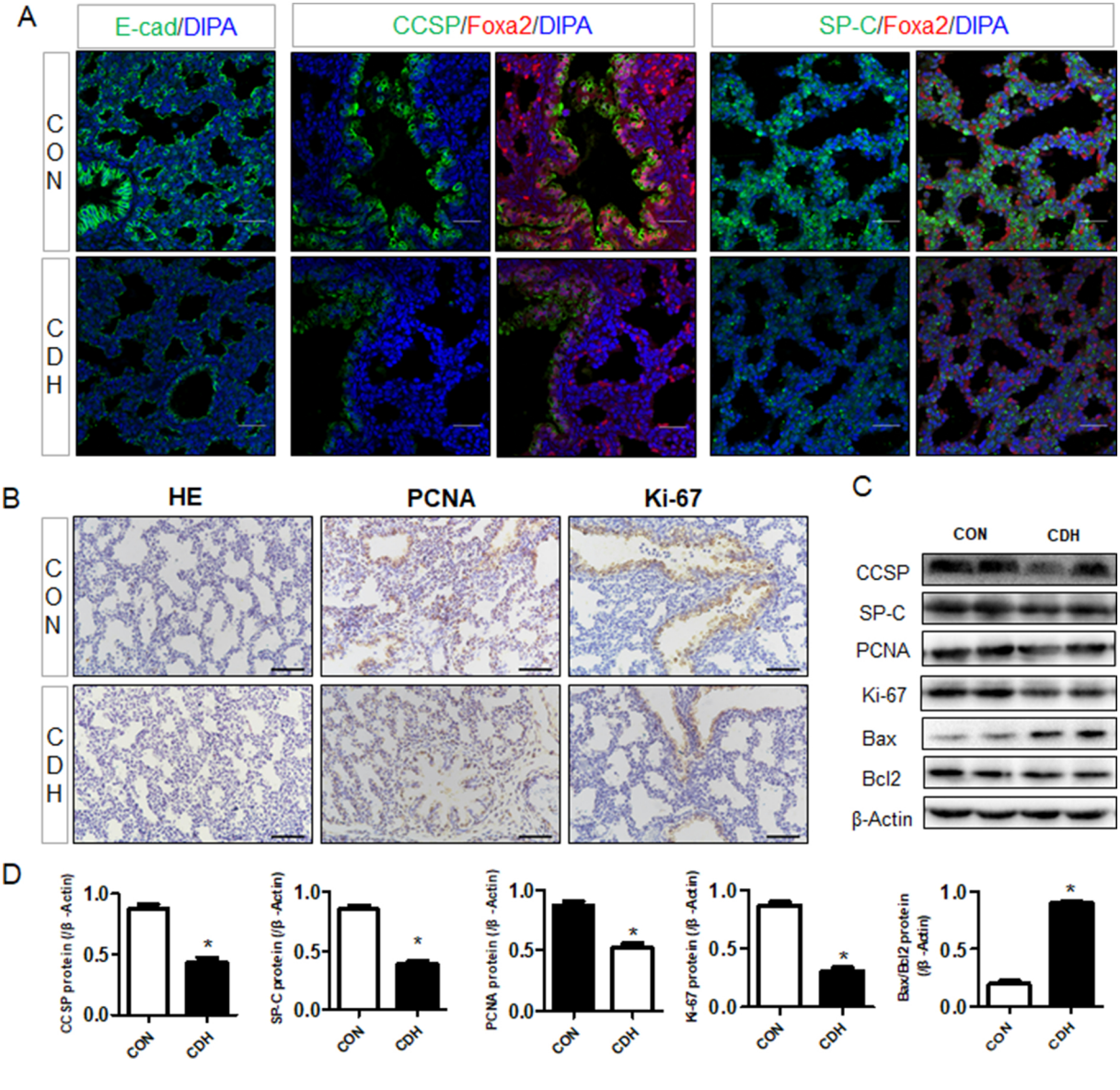
A
E-cad/DIPA
CCSP/Foxa2/DIPA
SP-C/Foxa2/DIPA
CON
CDH
B
HE
PCNA
Ki-67
CON
CDH
C
CON
CDH
CCSP
SP-C
PCNA
Ki-67
Bax
Bcl2
β-Actin
D
CCSP protein (/β -Actin)
SP-C protein (/β -Actin)
PCNA protein (/β -Actin)
Ki-67 protein (β -Actin)
Bax/Bcl2 protein (/β -Actin)
1.0
0.5
0.0
*
CON
CDH

Figure 2

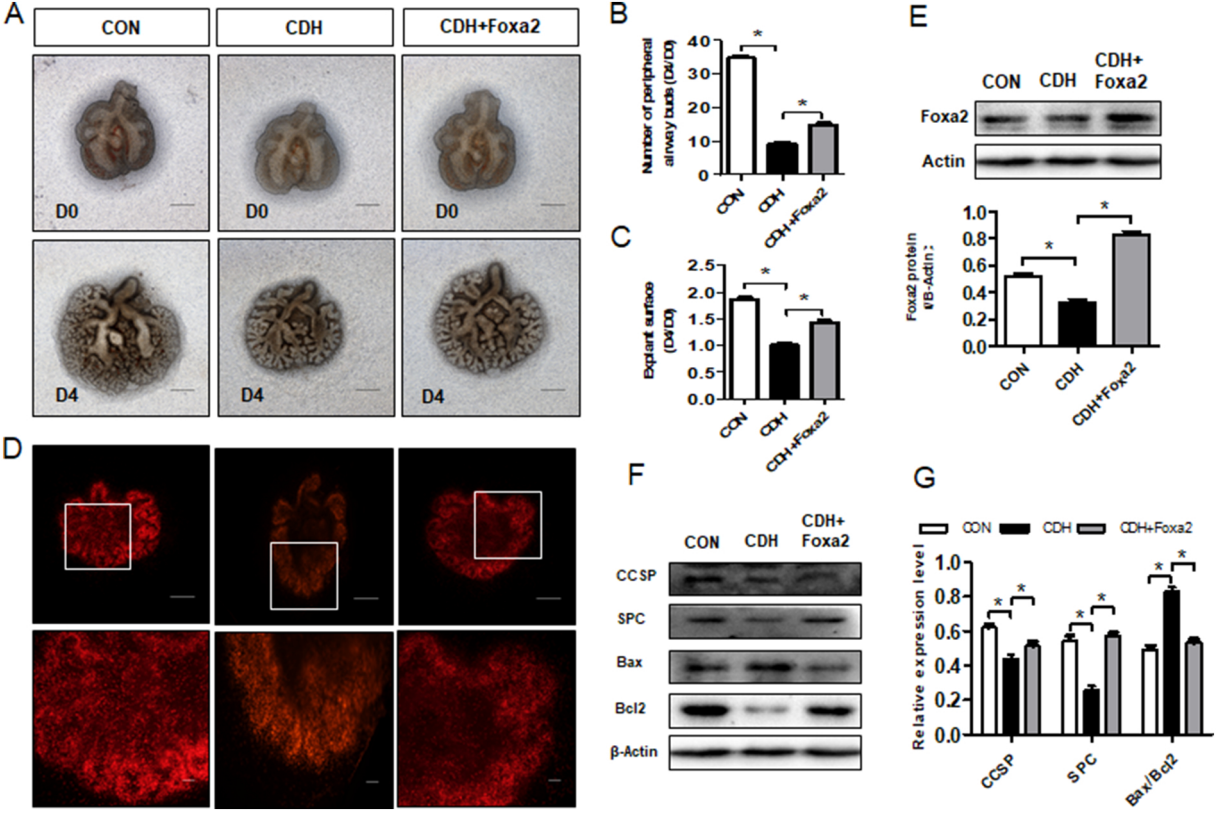
A
CON
CDH
CDH+Foxa2
D0
D0
D0
D4
D4
D4
B
Number of peripheral airway buds (D4/D0)
40
30
20
10
0
*
*
CON
CDH
CDH+Foxa2
C
Explant surface (D4/D0)
2.5
2.0
1.5
1.0
0.5
0.0
*
*
CON
CDH
CDH+Foxa2
D
E
CON
CDH
CDH+ Foxa2
Foxa2
Actin
Foxa2 protein WB-Actin:
1.0
0.8
0.6
0.4
0.2
0.0
*
*
CON
CDH
CDH+Foxa2
F
CON
CDH
CDH+ Foxa2
CCSP
SPC
Bax
Bcl2
β-Actin
G
CON
CDH
CDH+Foxa2
Relative expression level
1.0
0.8
0.6
0.4
0.2
0.0
* * * * * *
CCSP
SPC
Bax/Bcl2

Figure 3

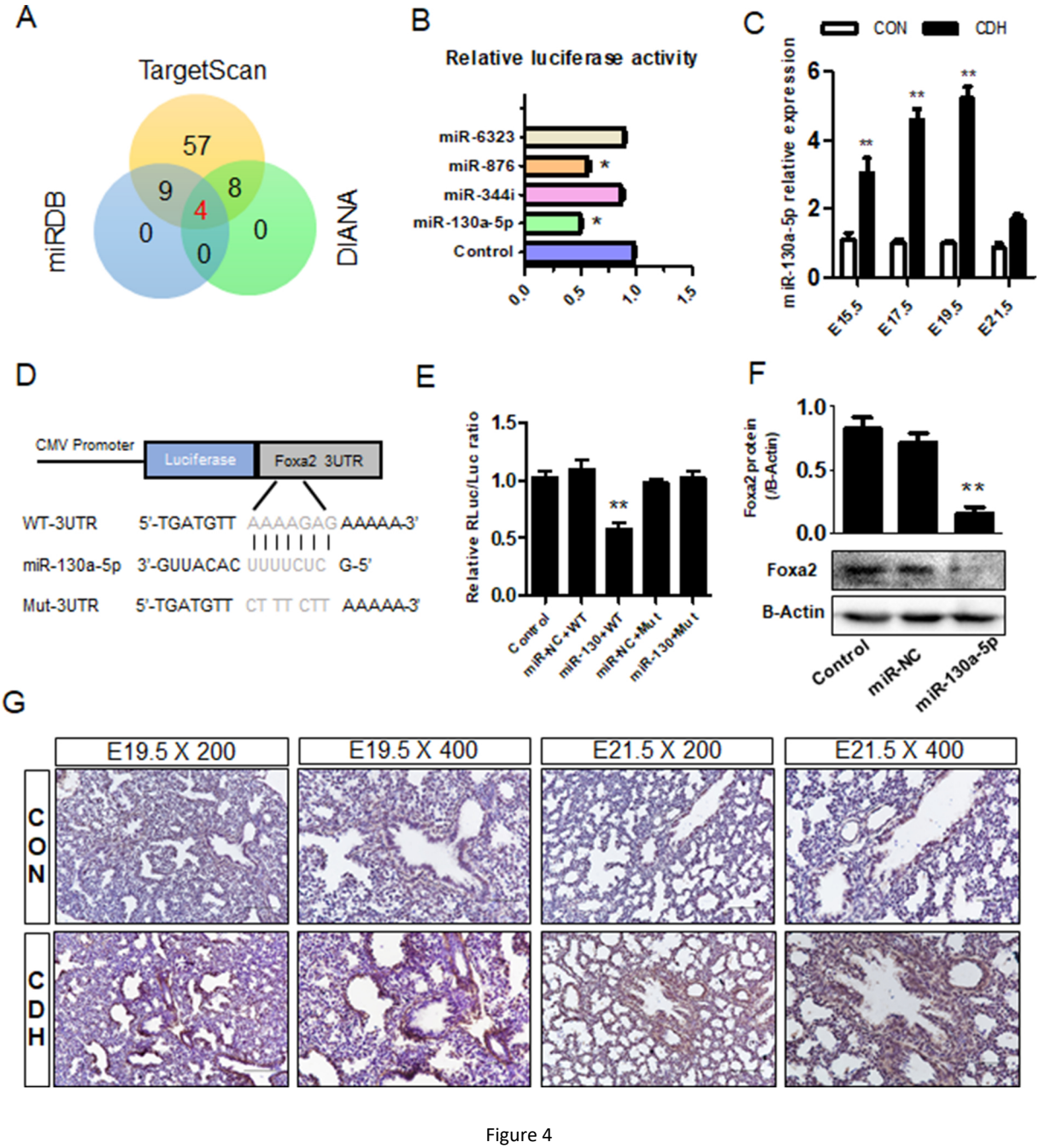
A
TargetScan
57
9
8
4
0
0
0
miRDB
DIANA
B
Relative luciferase activity
miR-6323
miR-876
miR-344i
miR-130a-5p
Control
0.0
0.5
1.0
1.5
C
CON
CDH
miR-130a-5p relative expression
E15.5
E17.5
E19.5
E21.5
D
CMV Promoter
Luciferase
Foxa2 3UTR
WT-3UTR 5'-TGATGTT AAAAGAG AAAAA-3'
miR-130a-5p 3'-GUUACAC UUUUCUC G-5'
Mut-3UTR 5'-TGATGTT CT TT CTT AAAAA-3'
E
Relative RLuc/Luc ratio
Control
miR-NC+WT
miR-130+WT
miR-NC+Mut
miR-130+Mut
F
Foxa2 protein (/B-Actin)
Foxa2
B-Actin
Control
miR-NC
miR-130a-5p
G
E19.5 X 200
E19.5 X 400
E21.5 X 200
E21.5 X 400
CON
CDH

Figure 4

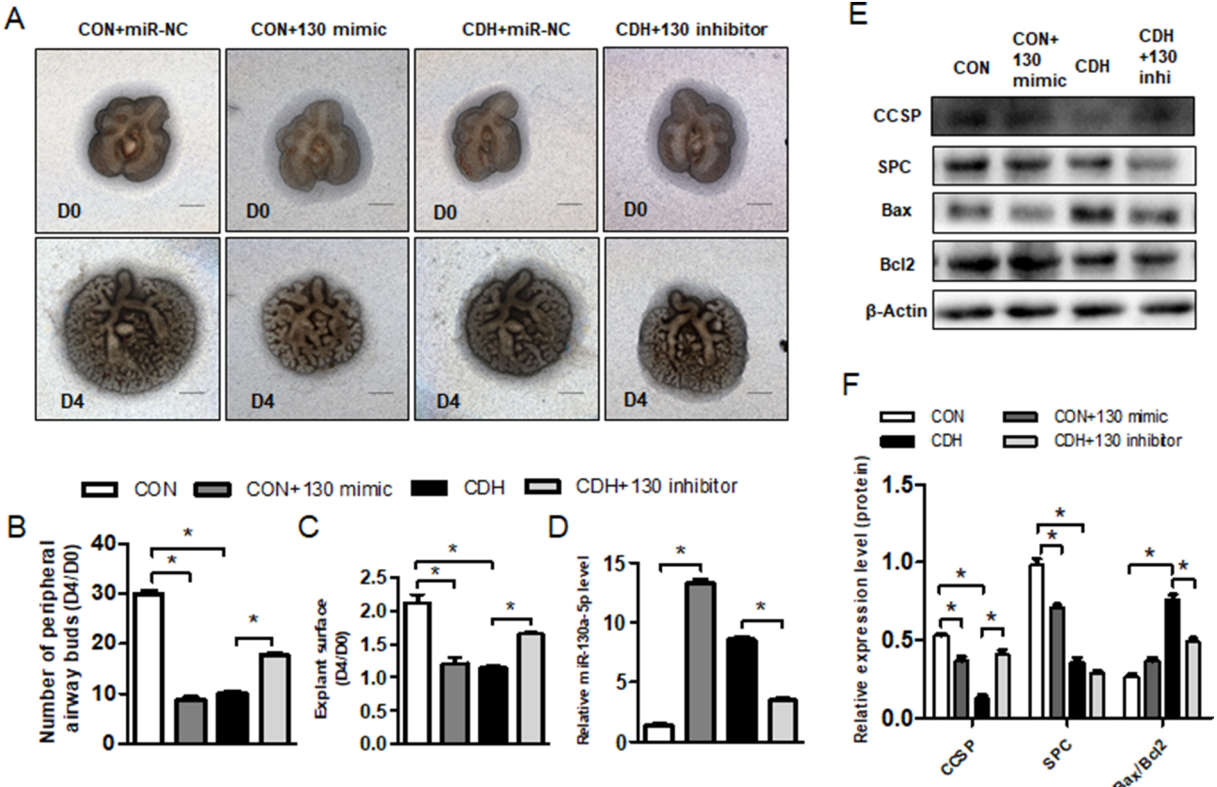
A
CON+miR-NC
CON+130 mimic
CDH+miR-NC
CDH+130 inhibitor
D0
D4
B
Number of peripheral airway buds (D4/D0)
C
Explant surface (D4/D0)
D
Relative miR-130a-5p level
CON
CON+130 mimic
CDH
CDH+130 inhibitor
E
CON
CON+ 130 mimic
CDH
CDH +130 inhi
CCSP
SPC
Bax
Bcl2
β-Actin
F
Relative expression level (protein)
CCSP
SPC
Bax/Bcl2

Figure 5

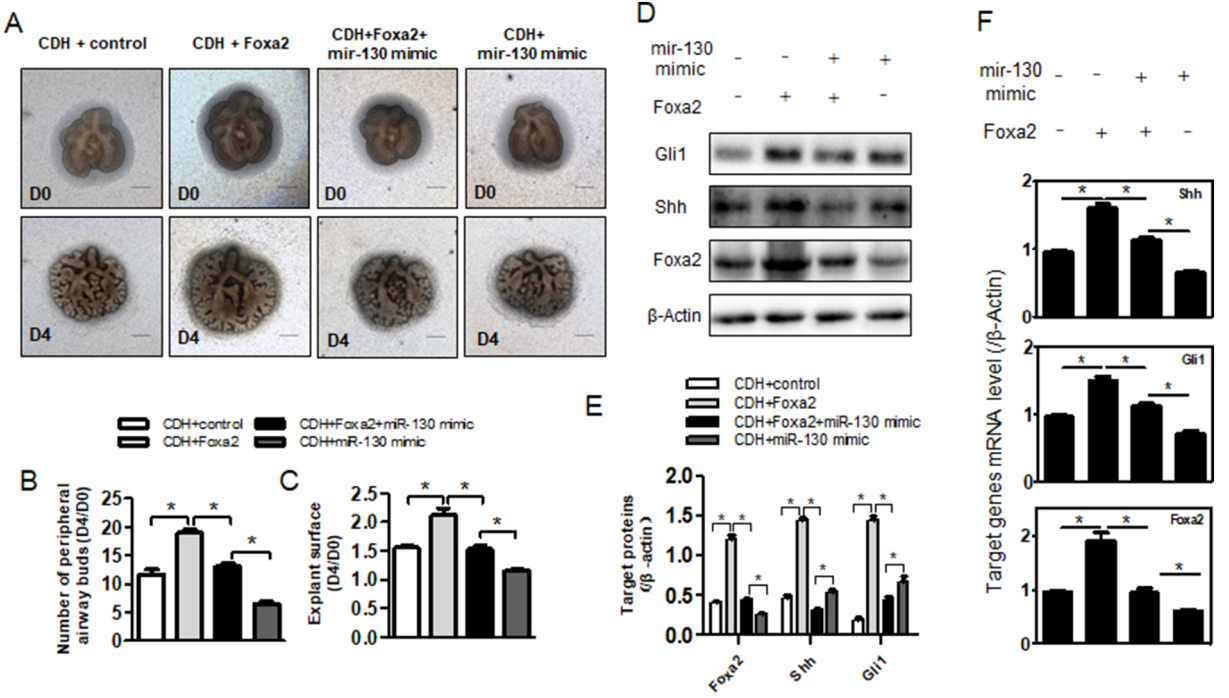
A
CDH + control
CDH + Foxa2
CDH+Foxa2+ mir-130 mimic
CDH+ mir-130 mimic
D0
D4
D
mir-130 mimic
Foxa2
Gli1
Shh
Foxa2
β-Actin
F
mir-130 mimic
Foxa2
Shh
Gli1
Foxa2
Target genes mRNA level (/β-Actin)
CDH+control
CDH+Foxa2
CDH+Foxa2+miR-130 mimic
CDH+miR-130 mimic
B
Number of peripheral airway buds (D4/D0)
C
Explant surface (D4/D0)
E
Target proteins (/β -actin)
Foxa2
Shh
Gli1

Figure 6